RESEARCH ARTICLE

Editorial Process: Submission:03/03/2025 Acceptance:11/17/2025 Published:11/21/2025

Dosimetric and Secondary Cancer Risk Comparison after Radiation Therapy for Breast Cancer with Three-Dimensional Conformal Radiotherapy, and Helical Tomotherapy

Shaghayegh Kamian^{1*}, Naeimeh Hashemi², Ahmad Mostaar³, Amir Bahador Yeke Dehghan³, Forough Farkhondeh³

Abstract

Background: This study aimed to compare the dose distribution and excess absolute risk (EAR) of secondary cancer risk for women with left breast cancer treated with mastectomy who were candidates for adjuvant radiotherapy between three-dimensional conformal radiotherapy (3D-CRT) and helical therapy (HT) techniques. Methods: For each patient planed with 3D-CRT, a plan was created for HT treatment, and data concluding maximum dose (D____,), mean dose (D_{mean}) , V_5 , V_{10} , V_{20} , and V_{30} were extracted from treatment planning systems. Organ equivalent dose (OED) and EAR were calculated based on the extracted data from dose-volume histogram (DVH). Results: In terms of D_{max}, HT technique showed lower values for the heart, spinal cord, and ipsilateral lung compared to 3D-CRT technique. For the thyroid, esophagus, contralateral breast and lung, 3D-CRT technique yielded lower D_{max} values. For D_{mean} , HT technique showed lower values only for the ipsilateral lung, while 3D-CRT technique produced lower values for the remaining organs. For V₅, V₁₀, V₂₀, and V₃₀, 3D-CRT technique generally exhibited lower values compared to HT technique, except the ipsilateral lung, where HT technique displayed lower values for V₁₀, V₂₀, and V₃₀. For the heart, HT technique showed lower values for V₂₀ and V₃₀. As a result, HT technique resulted in higher OEDs and EARs for the contralateral breast and lung, while 3D-CRT technique produced higher OEDs and EARs for the ipsilateral lung. Conclusions: HT and 3D-CRT exhibit varying efficacies in treating breast cancer patients, with HT demonstrating superior outcomes for sparing the heart and ipsilateral lung, while 3D-CRT holds an edge in minimizing dose to the contralateral breast and lung. The choice of the most appropriate radiation therapy technique for a particular patient should be made on a case-by-case basis, respecting the risk of secondary cancer development, pneumonitis, radiationinduced cardiac events, age, overall health.

Keywords: Breast neoplasm- Dose- Secondary Cancer- Radiotherapy

Asian Pac J Cancer Prev, 26 (11), 4009-4019

Introduction

In radiotherapy treatment, healthy tissues are also irradiated in addition to the target tissue; therefore, the risk of a radiation-induced second cancer potentially increases [1, 2]. The relationship between cancer risk and radiation dose is a complex one that has been the subject of much research. There is no clear consensus on whether the relationship is linear or nonlinear, and there is evidence to support both models [3]. Breast cancer accounting for 23% of all cancer cases and 14% of the cancer deaths worldwide is the most prevalent and common cancer in women and the major cause of cancer death among them [4]. In the

treatment procedure, Adjuvant radiotherapy following breast cancer surgery has a significant role in improving local control and overall survival [5-9]. However, studies have shown that women under 40 years old have an increased risk of developing secondary cancer following radiotherapy [10, 11]. Also, Promising advancements in early detection and treatment approaches have led to a growing population of long-term cancer survivors [2].

Different institutions may employ various radiotherapy techniques for breast cancer treatment [12]. In the center where the research was done, both 3D-CRT and IMRT techniques utilized. For IMRT, a Tomotherapy system with Helical delivery method employed. In Helical

¹Department of Radiation Oncology, School of Medicine, Imam Hossein Hospital, Shahid Beheshti University of Medical Sciences, Tehran, Iran. ²Department of Radiation Oncology, School of Medicine, Shahid Beheshti University of Medical Sciences, Tehran, Iran. ³Department of Medical Physics and Biomedical Engineering, School of Medicine, Shahid Beheshti University of Medical Sciences, Tehran, Iran. *For Correspondence: shkamian@sbmu.ac.ir

tomotherapy, the patient translates longitudinally through the treatment field while radiation is delivered via rotating fan beams [7] and Due to the rotational delivery of Helical tomotherapy, multiple beams traverse through normal tissue regions previously unexposed to radiation with the fixed angles of 3DCRT [7].

New irradiation techniques have varying effects on the amount of radiation dose delivered to different body structures, consequently, have differences risk of radiationinduced secondary cancer [6, 9, 10, 13, 14].

IMRT offers advantages over 3D-CRT, including reducing the dose to surrounding normal tissue. However, a primary disadvantage of IMRT is the increased out-offield leakage radiation and scattering due to the increased monitor units and higher number of fields and significantly increasing the volume that receives low-dose radiation [11, 13, 15, 16] Additionally, the beam-limiting devices, leakage radiation, and secondary radiation produced by any object in the primary beam can contribute to patient exposure [16, 17]. This might increase the risk for secondary malignancies [11, 18], which regarding the life expectancy, for patients with breast cancer is a very important issue [10]. Based on biological models, from dose-volume histograms (DVH) the excess absolute risk (EAR) of a second cancer occurring after exposure to radiation can be estimated [6]. The EAR is used to quantify the increased risk of developing a secondary cancer in individuals exposed to radiation compared to the general population. This risk is expressed per 10,000 personyears and is calculated based on the organ equivalent dose (OED) [19].

Many studies have compared treatment methods like 3D-CRT, with more advanced methods, like IMRT and VMAT [2, 9-12, 20-22].

Purpose

In this study, as mentioned earlier, based on the dose-volume histogram curves, the dose reached to the organs was evaluated; And finally, on the basis of biological models provided by the BEIR (biological effects of ionizing radiation) VII model [23], the possibility of secondary malignancy for 3D-CRT and IMRT (Helical-Therapy which used HT as abbreviation) modalities was measured in the opposite breast and lungs on both sides based on the concept of OED, EAR and EAR_{main} for the linear-exponential, plateau, and full mechanistic doseresponse models.

Materials and Methods

This study evaluated 10 female patients with left breast cancer treated with modified radical mastectomy who were candidates for adjuvant radiotherapy which their clinical stages are mentioned in Table 1. The age of cases were 28-79 years old with the average of 55 years. All patients received 50 Gy in 25 fractions and their information detailed in Table 1. Treatment was delivered using Elekta Compact (Stockholm, Sweden) and Varian 2300 C/D (Palo Alto, California, USA) machines in 3D-CRT modality. The treatment plans were compared with HT plans generated using Accuray Precision (Madison, United

States) software for the Tomotherapy system.

The dose to the organs was measured based on the dose-volume histogram (DVH) curves, based on the following parameters: mean dose ($D_{\rm mean}$), maximum dose ($D_{\rm max}$), and VX (the volume of the organ that receives at least X Gy) for V_5 , V_{10} , V_{20} , and V_{30} .

Also, in Precision TPS Conformity Index (CI) and Homogeneity Index (HI) for each HT plan checked out and results mentioned in next section. The Conformity Index was defined by Paddick [24] as shown in Formula 1, where V_{T,P_i} is the volume of target enclosed by the prescription dose, V_{P_i} is the volume of tissues including target covered by the prescription dose, and VT is the volume of target. The Homogeneity Index was defined as the ratio of the difference between the dose to the 5% volume ($D_{5\%}$) and the 95% volume ($D_{95\%}$) to the D_{mean} , expressed as a percentage (Formula 2) [25].

$$CI = \frac{V_{T,Pi} \times V_{T,Pi}}{V_T \times V_{Pi}} \tag{1}$$

$$HI = \frac{D_{5\%} - D_{95\%}}{D_{Mean}} \times 100 \tag{2}$$

All patients underwent CT (Siemens, Somatom, Erlangen, Germany) simulation according to departmental protocols, with 5 mm slices in the supine position on the breast board, with the arm on the side of the affected breast placed above the head. Treatment plans were created for all patients in the Isogray 4.2.3 (3D-CRT) and Precision 2.0.1.1 (Helical-Therapy) treatment planning systems (TPSs), considering the dose received by the clinical target volume (CTV) and the organs at risk (OARs), including the thyroid, opposite breast, lungs, esophagus, heart, and spinal cord. All structures were contoured by radiation oncologist according to the Radiation Therapy Oncology Group (RTOG) guidelines. The clinical target volume included the chest wall and regional lymph nodes (axillary, infraclavicular, and supraclavicular), and the planning target volume included the CTV plus a 5 mm margin.

The goal was to cover at least 95% of the PTV with at least 95% of the prescribed dose. Dose constraints for the lung on the treatment side were a mean dose below 20 Gy and a volume that receives at least 20 Gy (V_{20}) below 30%. For the heart, the D_{mean} was below 10 Gy and the V_{20} was below 15%. For the spinal cord, the D_{max} was 45 Gy. The dose for the opposite breast and lung was kept as low as possible without compromising the dose to the target volume of the treatment. And for the esophagus, the

Table 1. Clinical Stage Information of Patients Examined with Tomotherapy and 3D-CRT Techniques.

Clinical stage information								
Stage (N) Abundance Stage (T) Abunda								
0	1	1	0					
1	6	2	3					
2	1	3	4					
3	2	4	3					

 $\boldsymbol{D}_{\text{mean}}$ was kept below 34 Gy.

Finally, the risk of secondary malignancy in the opposite breast and lungs on both sides was measured using the Schneider's concept of OED [23]. To estimate and compare the risk of secondary malignancy following radiotherapy, the concept of Organ Equivalent Dose (OED) was used. OED, introduced by Schneider [5], includes the effect of treatment session (fractionation) and parameters of repair and repopulation. Based on the concept of OED, two different radiotherapy plans with equal risk of secondary malignancy have equal OED [5]. The OED for the opposite breast and lungs was calculated based on the DVH curves, as follows:

Assuming a linear dose-response relationship with the exposure dose:

$$OED_{lin} = \frac{1}{V_0} \sum_{i} V_{Di} D_i \tag{3}$$

Considering that the probability of cell death increases exponentially with the dose, and thus the risk of developing cancer due to mutant cell death may decrease:

$$OED_{linear-exp} = \frac{1}{V_0} \sum_{i} V_{Di} Di \exp(-\alpha' Di)$$
 (4)

If it is assumed that due to the balance between cell death and secondary cell recovery relative to the fractionated treatment scheme, the dose-response reaches a plateau after a linear increase up to a certain dose:

$$OED_{plateau} = \frac{1}{V_0} \sum_{i} V_{Di} \frac{1 - \exp(-\alpha' Di)}{\alpha'}$$
 (5)

And finally, when the plateau and exponential linear models are evident and considering the number of treatment sessions:

 $OED_{mechanistic}$

$$= \frac{1}{V_0} \sum_{i} V_{Di} \frac{\exp(-\alpha'Di)}{\alpha'R} \tag{6}$$

$$+ \left[1 - 2R + R^2 \exp(\alpha' Di) - (1 - R)^2 \exp\left(-\frac{\alpha' R}{1 - R} Di\right)\right]$$

In the formula (6), V_0 is the total volume of the organ. V_{Di} , the volume of the organ exposed to the radiation dose D_i . And, α' and R, organ-specific parameters derived from data from atomic bomb survivors and patients with Hodgkin's disease treated with radiotherapy which displayed in Table 2.

Then, the Excess Absolute Risk (EAR) was employed

to determine the likelihood of developing a secondary malignancy subsequent to radiotherapy. The EAR represents the absolute difference in the incidence of malignancy between individuals exposed to dose d and those not exposed, expressed per 10,000 person-years per Gy. The EAR is calculated using formula (7):

$$EAR = 0ED\beta' exp \left[\gamma_e (agex - 30) + \gamma_a ln \left(\frac{agea}{70} \right) \right]$$
 (7)

The parameters used in the formula (7) are derived from Schneider's data(3). agex represents the patient's age at the time of radiation exposure, while agea denotes the patient's anticipated lifespan. Based on previous studies, we have assumed a maximum lifespan of 70 years for our calculations.

Key parameters in EAR_0 (the slope of the dose–response curve at a low dose) include the type of affected organ, the patient's age at the time of exposure, their sex, and their expected lifespan. These parameters are extracted from Schneider's (3) data, and we assume that patients encounter radiotherapy at the age of 30 and live to reach the age of 70.

$$EAR = EAR_0 \times OED \tag{8}$$

Statistical analyses were conducted using IBM SPSS Statistics version 22 software. The "Shapiro-Wilk" test was employed to evaluate the normality of continuous data and "t test" was used for comparisons. Mean and standard deviation were used to describe quantitative data with normal distribution, and median and interquartile range were used to describe quantitative data with nonnormal distribution. Categorical data were presented as frequencies and percentages, and frequency tables and graphs were employed to visualize the data distribution. A P-value of less than 0.05 was considered statistically significant.

Results

A total of 10 patients were treated using the 3D-CRT technique. Three patients were treated with an Elekta Compact machine, while the remaining seven patients were treated with a Varian 2300 C/D machine. All treatment plans were generated using the Isogray TPS. Additionally, treatment plans were created for all patients using the Precision TPS (Figure 1), which resulted in an average treatment time of 399.8 \pm 60.71 seconds. Also, some dose indicators of target in HT technique displayed in Table 3. For these plans, the minimum and maximum Conformity Index values were 1.05 and 1.32, respectively, with an average value of 1.16. The minimum and maximum Homogeneity Index values were 1.11 and

Table 2. Parameters for Second Malignancy Risk Calculation [3, 10]

Site	EAR ₀	"Linear-Exponential" Model	"Plateau" Model	"Full Mechan	nistic" Model
	$\alpha'(\mathrm{Gy^{-1}})$		α' (Gy ⁻¹)	α' (Gy ⁻¹)	R
Female Breast	8.2	0.041	0.115	0.044	0.15
Lung	8	0.022	0.056	0.042	0.83

(a)

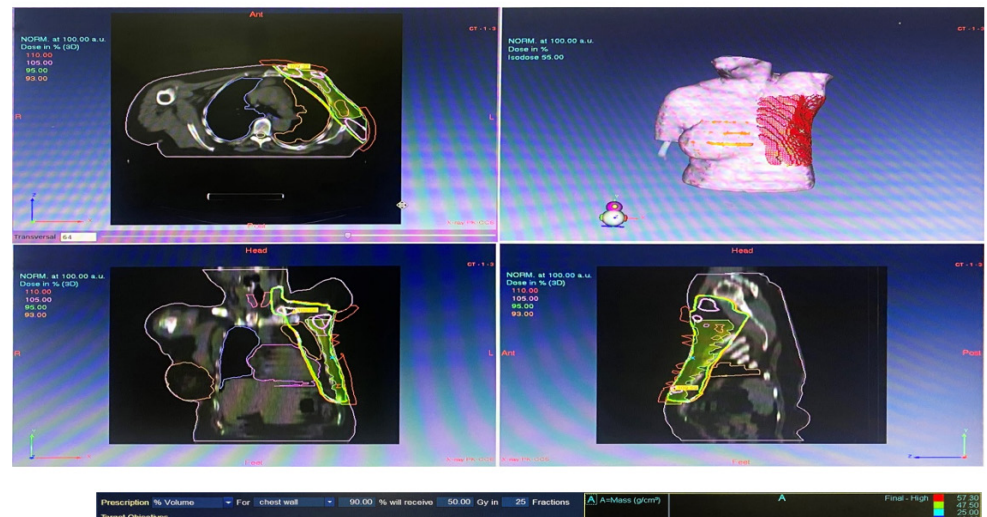




Figure 1. The Isodose Distribution for the Two Plans in Axial Plane for a Representative Patient (a) 3DCRT; (b) Tomotherapy

1.16, respectively, with an average value of 1.13.

The parameters related to the received dose of organs at risk and the risk of secondary cancers were compared between 3D-CRT and HT techniques as follows:

In the heart, the D_{max} , V_{20} , and V_{30} were significantly higher in the 3D-CRT technique than in HT. However, V_5 and V_{10} were significantly higher in HT. The D_{mean} did not differ between the two techniques. All dosevolume parameters were significantly higher in the HT technique for the thyroid. Also, In the esophagus, all dose parameters, with the exception of V_{30} , were significantly higher in the HT technique. The D_{mean} , V_5 , and V_{10} were all significantly lower in 3D-CRT technique than in HT for the spinal cord. However, there was no significant difference in V_{20} , V_{30} , or the D_{max} .

The D_{max} , D_{mean} , V_5 , and V_{10} were all significantly lower in three-dimensional technique than in HT for the contralateral lung. However, there was no significant difference in V_{20} , and V_{30} was zero for both techniques. In contrast, for the ipsilateral lung, D_{mean} , V_{20} , and V_{30} were all significantly higher in 3D-CRT than in HT technique. However, there was no significant difference in V_{10} or the D_{max} and compared to the 3D-CRT, V_5 values were marginally higher in the HT technique.

The contralateral breast exhibited near-identical characteristics to the contralateral lung, except for V_{20} and V_{30} values. The D_{max} , D_{mean} , V_{5} , and V_{10} were significantly lower when utilizing three-dimensional technique compared to Tomotherapy. However, V_{20} did not exhibit a statistically significant difference. Additionally, V_{30} was

Table 3. Dose Indicators of Target Volume Related to Treatment Planning with HT Technique

Target related contours volume	Mean	Standard deviation	Minimum	Maximum
PTV V _{100%}	83.44	8.67	62.9	90.9
PTV V _{95%}	96.99	1.66	95.3	99.4
PTV V _{90%}	98.9	0.74	97.9	99.9
CTV V _{98%}	97.62	2.11	94.2	99.9
CTV V _{95%}	99.26	0.98	97.4	100

Y V_{x%} = volume of Y target which receive at least X% of prescription dose

zero for both techniques. All related data is displayed in Table 4 in detail.

All metrics related to secondary malignancies, including the OED, EAR (assuming all patients received radiotherapy at age 30 and lived to age 70 to nullify the influence of age) and EAR_{main} (taking into account the actual age of patients at the time of radiotherapy and their potential lifespan of up to 70 years), demonstrated higher values for the contralateral breast and lung when employing the HT technique.

Figure 2 exhibits the D_{mean}, OEDs, EARs, and EAR_{main}s for both techniques. The calculated OEDs for both techniques in the contralateral breast, ipsilateral lung, and

contralateral lung are superior to the D_{mean} . In 3D-CRT, the gap between the OEDs and D_{mean} for the contralateral breast and contralateral lung is smaller than in HT. On the contrary, the opposite is true for the ipsilateral lung and the difference between the OEDs and the D_{mean} for HT was less than that in 3D-CRT. More detailed data is displayed in Tables 5 and 6.

The contralateral breast and lung received higher equivalent doses (OEDs) with intensity-modulated radiation therapy compared to 3D-CRT. Conversely, the ipsilateral lung received lower OEDs with HT compared to 3D-CRT. Similar to OEDs, equivalent absorbed doses (EARs) for the contralateral breast and lung were

Table 4. Comparison of Heart, Thyroid, Esophagus, Spinal Cord, Contralateral Breast, Contralateral Lung and Ipsilateral Lung Dose-Volume Metrics as a Function of Plan Modality ("x ± sd)

Modality	D _{max}	D _{mean}	V ₅ (%)	V_{10} (%)	$V_{20}(\%)$	V_{30} (%)
Heart						
HT	46.53 ± 4.19	7.44 ± 1.34	48.40 ± 16.30	23.24 ± 5.52	6.95 ± 1.50	2.08 ± 0.96
3D-CRT	51.58 ± 3.60	7.42 ± 1.34	22.50 ± 6.39	15.20 ± 3.77	11.56 ± 2.17	9.17 ± 1.99
P-value	0.01	0.984	0.001	0.001	< 0.001	< 0.001
Thyroid						
HT	52.99 ± 0.78	32.53 ± 3.60	100	98.06 ± 4.94	76.43 ± 21.21	48.39 ± 7.27
3D-CRT	48.95 ± 5.29	17.00 ± 6.82	47.94 ± 7.92	40.55 ± 9.38	32.22 ± 14.29	27.06 ± 17.27
P-value	0.04	< 0.001	< 0.001	< 0.001	< 0.001	0.004
Esophagus						
HT	51.87 ± 5.30	12.71 ± 3.43	48.63 ± 11.79	35.26 ± 10.95	23.64 ± 9.25	16.68 ± 8.47
3D-CRT	42.01 ± 7.67	6.43 ± 3.98	23.43 ± 9.71	17.09 ± 11.67	11.81 ± 11.49	8.65 ± 9.63
P-value	0.004	0.001	< 0.001	0.002	0.021	0.063
Spinal Cord						
HT	27.95 ± 7.68	6.73 ± 1.16	41.26 ± 5.08	23.59 ± 3.55	7.77 ± 6.28	1.90 ± 4.04
3D-CRT	30.77 ± 12.94	3.19 ± 2.04	13.00 ± 7.18	7.68 ± 7.26	4.97 ± 5.98	2.73 ± 4.90
P-value	0.562	< 0.001	< 0.001	< 0.001	0.321	0.686
Contralateral breast						
HT	18.29 ± 8.26	3.49 ± 1.18	17.28 ± 15.42	1.43 ± 1.91	0.06 ± 0.16	0
3D-CRT	4.67 ± 2.37	0.27 ± 0.17	0	0	0	0
P-value	< 0.001	< 0.001	0.006	0.042	0.26	-
Contralateral lung						
HT	21.60 ± 4.59	4.39 ± 1.03	33.45 ± 12.36	7.23 ± 3.78	0.06 ± 0.11	0
3D-CRT	9.23 ± 13.06	0.61 ± 0.24	0.36 ± 1.13	0	0	0
P-value	0.011	< 0.001	< 0.001	< 0.001	0.111	-
Ipsilateral lung						
HT	52.56 ± 2.07	12.63 ± 1.36	63.11 ± 7.89	40.18 ± 5.08	22.01 ± 3.12	12.72 ± 2.74
3D-CRT	53.65 ± 3.25	18.31 ± 3.35	59.67 ± 6.09	44.96 ± 7.31	35.62 ± 7.20	31.00 ± 6.97
P-value	0.381	< 0.001	0.29	0.107	< 0.001	< 0.001

 $D_{\text{\tiny max}}, \text{ maximum dose; } D_{\text{\tiny mean}}, \text{ mean dose; Gy, Gray; Vx, volume (\%) receiving x dose (Gy) or higher.}$

Table 5. OED for Contralateral Breast, Contralateral Lung and Ipsilateral Lung in HT and 3D-CRT

OED type	contralateral breast			Contralateral lung			Ipsilateral lung		
	HT 3D-CRT P-value			HT	3D-CRT	P-value	HT	3D-CRT	P-value
OED _{linear-exp}	5.43 ± 1.88	0.62 ± 0.44	< 0.001	8.64 ± 3.46	1.03 ± 0.38	< 0.001	23.04 ± 2.68	33.74 ± 7.98	0.002
OED _{plateau}	5.17 ± 1.76	0.61 ± 0.43	< 0.001	8.37 ± 3.28	1.02 ± 0.38	< 0.001	21.87 ± 2.55	32.07 ± 7.52	0.002
OED mechanistic	5.18 ± 1.75	0.61 ± 0.44	< 0.001	8.40 ± 3.33	1.02 ± 0.38	< 0.001	22.10 ± 2.59	32.60 ± 7.62	0.002

Table 6. EAR and EAR_{main} for Contralateral Breast, Contralateral Lung, Ipsilateral Lung in 3D-CRT and HT

EAR type	Contralateral breast			Contralateral lung			Ipsilateral lung		
	HT	3D-CRT	P-value	HT	3D-CRT	P-value	HT	3D-CRT	P-value
EAR _{linear-exp}	44.55 ± 15.43	5.07 ± 3.59	< 0.001	69.08 ± 27.68	8.23 ± 3.05	< 0.001	184.32 ± 21.43	269.89 ± 63.82	0.002
$EAR_{plateau}$	42.42 ± 14.42	4.97 ± 3.52	< 0.001	66.95 ± 26.23	8.14 ± 3.01	< 0.001	174.94 ± 20.41	256.58 ± 60.12	0.002
EAR	42.45 ± 14.50	5.00 ± 3.55	< 0.001	67.90 ± 26.80	8.18 ± 3.02	< 0.001	178.10 ± 20.82	260.10 ± 60.90	0.002
$\mathrm{EAR}_{\mathrm{main.linear-exp}}$	27.86 ± 16.79	2.64 ± 2.53	< 0.001	67.98 ± 27.46	8.12 ± 3.02	< 0.001	181.35 ± 19.66	264.89 ± 57.37	0.001
$\mathrm{EAR}_{\mathrm{main.plateau}}$	26.49 ± 15.71	2.59 ± 2.48	< 0.001	65.88 ± 26.00	8.02 ± 2.99	< 0.001	172.12 ± 18.69	251.84 ± 54.07	0.001
EAR _{main.mechanistic}	26.58 ± 15.90	2.60 ± 2.50	< 0.001	66.12 ± 26.50	8.07 ± 3.00	< 0.001	175.90 ± 19.01	257.36 ± 55.3	0.001

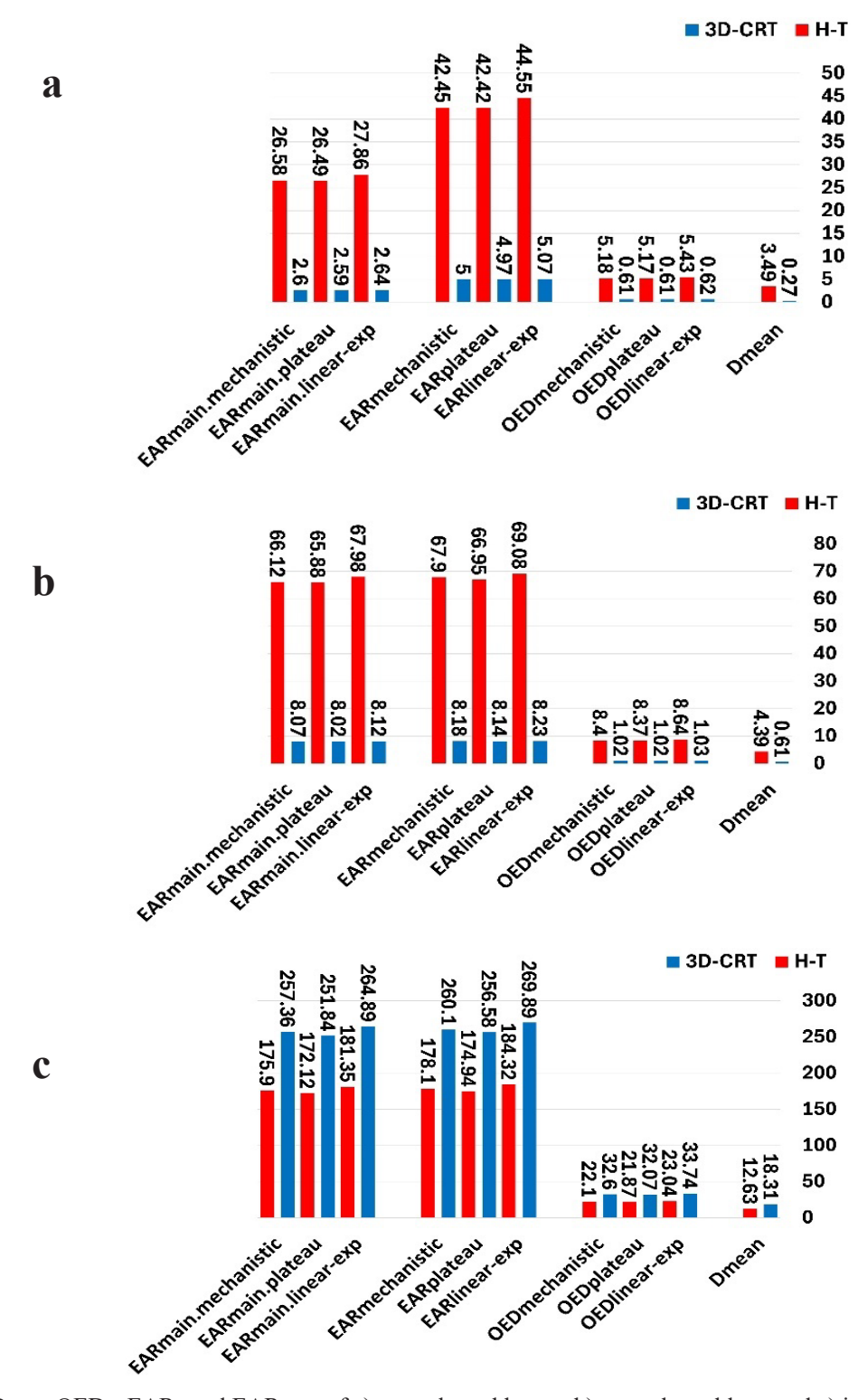


Figure 2: D $_{mean}$, OEDs, EARs and EAR $_{mains}$ of a) contralateral breast, b) contralateral lung and c) ipsilateral lung for HT and 3D-CRT which averaged over 10 patients' data

significantly higher with HT compared to 3D-CRT. In contrast, EARS for the ipsilateral lung were lower with HT compared to other techniques.

The trend was similar for EAR $_{\rm main}$ values, with EAR $_{\rm main}$ for the contralateral breast and lung being substantially higher with HT compared to 3D-CRT and lower for the ipsilateral lung. EAR $_{\rm main}$ and EAR values exhibited small differences, except for the contralateral breast in HT where EAR $_{\rm main}$ was nearly half the value of EAR.

Discussion

In breast cancer treatment using three-dimensional conformal radiotherapy (3D-CRT), tangential fields are often employed. These fields, including hard-wedge, dynamic-wedge, and field-in-field (FinF) techniques, are typically utilized for whole-breast irradiation to achieve more uniform tumor dose distribution [8, 26, 27]. The introduction of novel irradiation techniques like IMRT and VMAT may lead to variations in the overall radiation dose delivered to the patient's body, potentially influencing the risk of radiation-induced secondary cancers [14]. These new radiotherapy techniques have had excellent results in terms of dose conformity and uniformity to the target volume, compared to 3D-CRT [21]. However, the volume that receives low doses (low dose bath), such as the opposite breast and lungs, is significantly higher with these techniques than with 3D-CRT, which is associated with the risk of radiation-induced secondary malignancy [9, 10, 22]. Our study found that the results were consistent for the opposite breast and opposite lung, but there was no significant difference in the low dose received by the treated side lung. This is likely because the mentioned studies had access to three-dimensional treatment planning systems with MLCs, while our center does not. As a result, the dose for the treated side lung in our study was higher than in the other studies.

It should be noted, the dose calculations in this study were primarily based on commercially available treatment planning systems, which may introduce inherent limitations and potential inaccuracies. Monte Carlo methods are widely acknowledged as the most accurate dose calculation algorithms for both in-field and out-of-field dose estimations [28, 29]. Accordingly, this calculation algorithm was employed for Helical-Therapy planning. However, due to the absence of Monte Carlo calculations for 3D-CRT and wedge planning in commercial planning systems, the Collapsed Cone algorithm was utilized for this technique. While the Collapsed Cone algorithm has demonstrated established accuracy [30, 31], interpretation of the results obtained using the 3D-CRT technique should be approached with prudence. This is because non-Monte Carlo calculations can underestimate doses outside the treatment field and to contralateral structures by up to 50%, as evidenced by relevant studies [16, 32].

Our findings align with Schubert et al.'s [7] research, which indicated that HT delivered lower D_{max} to the heart and ipsilateral lung compared to 3D-CRT. However, our study revealed a slight difference in D_{mean} of heart, with HT administering a marginally higher dose (averagely

7.44 Gy for HT and 7.42 Gy for 3D-CRT). Conversely, the D_{mean} of ipsilateral lung was significantly lower with HT While, Abo-Madyan (2) results, which compared tangential 3D-CRT, tangential IMRT, multibeam IMRT, and VMAT for whole-breast treatment of left-sided breast cancer, show lower D_{mean} for ipsilateral lung in 3D-CRT compare to IMRT technique.

Haciislamoglu et al.'s [12] findings corroborate ours, reporting similar trends for the heart and ipsilateral lung. They found only a slight difference in D_{mean} of heart between the two modalities, with higher D_{max} to the heart and ipsilateral lung in 3D-CRT compared to HT. Also, in our study V₂₀ and V₃₀ of heart was lower with HT technique than 3D-CRT, but V_5 and V_{10} were significantly lower in three-dimensional which are identic with Haciislamoglu et al.'s(12) results. Must be notice, they reported lower D_{max} in Forward-IMRT, Inverse-IMRT and VMAT, higher D_{mean} in Inverse-IMRT and VMAT, higher V₅ in Inverse-IMRT and VMAT, higher V₁₀ in Forward-IMRT, Inverse-IMRT and VMAT, higher dose for V₂₀ in Forward-IMRT, Inverse-IMRT and VMAT, compared to 3D-CRT. In addition, Baycan et al. [8] reported lower V_5 , V_{10} , V_{20} and V_{30} in Field in field-IMRT against 3D-CRT for heart.

A study by Xie et al. [33] compared the mean and maximum doses delivered by conventional tangential and field-in-field 3D-CRT, Hybrid, IMRT, Standard-VMAT, Nonecoplanar-VMAT, and Multi arc-VMAT. They found that 3D-CRT techniques consistently delivered higher $D_{\rm mean}$ and $D_{\rm max}$ values than the advanced techniques. Our findings corroborate their results, but thier study also revealed a larger discrepancy in $D_{\rm mean}$ between 3D-CRT techniques and other techniques. In particular, both type of 3D-CRT techniques in their study delivered the highest $D_{\rm mean}$ value among all the techniques.

Several studies have demonstrated that the risk of radiation-induced pneumonitis strongly correlates with lung V_{10} and V_{20} values [34-37]. While Moon et al. [38] reported higher ipsilateral lung V_{10} and V_{20} values for Tomotherapy compared to 3D-CRT in their study of lumpectomy cases, our findings differ significantly. In our study, patients treated with 3D-CRT exhibited higher values for both metrics: 44.96% and 35.62%, respectively, compared to 40.18% and 22.01% for HT technique. These findings suggest potential benefits of Tomotherapy system and HT technique in minimizing radiation-induced lung complications.

The D_{max} and D_{mean} to both the contralateral lung and contralateral breast were higher in HT technique compared to 3D-CRT, which aligns with the findings of Haciislamoglu et al. [12] in their study of lumpectomy cases. Schubert et al. [7] also observed similar trends for the contralateral lung, but they found that Tomotherapy resulted in lower D_{max} to the contralateral breast compared to 3D-CRT.

In this study, align with other studies [12] while $\rm V_5$ for the contralateral breast and lung were 0% and 0.36% with 3D-CRT, these values were 17.28% and 33.45% with Tomotherapy, respectively, which were significantly higher.

Furthermore, all dose parameters for the thyroid gland and all but V₃₀ for the esophagus were higher in Asian Pacific Journal of Cancer Prevention, Vol 26 **4015**

HT. This can likely be attributed to two factors: first, a 5-millimeter margin was added to the PTV for the axillary and supraclavicular lymph nodes in Tomotherapy treatment planning, whereas no such margin was utilized in 3D-CRT. Second, the specific characteristics of the Tomotherapy system, including its helical delivery with 51 projections, can lead to trade-offs between optimal dose homogeneity and conformity in certain target volumes, potentially explaining the higher doses to these organs. Notably, a thyroid shield was employed in all 3D-CRT patients, further influencing dose distribution.

Alongside efforts to mitigate acute and late toxicities through dose-volume tolerance studies and acceptable limits for ipsilateral and contralateral structures, a comprehensive assessment of radiation-induced secondary cancer risk is paramount. Several mathematical models have been developed to estimate this risk, while the EAR provides a more refined representation of the doseresponse relationship, considering the age at exposure, the attained age, and a more detailed depiction of the relationship between dose and risk. For lower doses (less than 2 Gy), the dose-risk relationship is linear for all solid organs. However, it is postulated that the risk of cancer induction diminishes at higher doses (up to 40 Gy) due to a complex interplay between cell killing and repopulation effects [19].

This study compared the Excess Absolute Risk (EAR) of secondary cancer development in the contralateral breast and lungs between Tomotherapy and 3D-CRT techniques. As expected based on previous research [9, 10], Tomotherapy resulted in higher EAR values for both the contralateral breast and lung, suggesting a potentially increased risk. However, for the ipsilateral lung, 3D-CRT unexpectedly exhibited higher EAR values, contradicting existing findings. Interestingly, the findings of Zhang et al.'s study [19] employing the Hybrid-VMAT technique corroborate our observed higher EAR with 3D-CRT for the ipsilateral lung.

This anomaly might be attributed to the lack of a multileaf collimator (MLC) in our facility and the ipsilateral lung, positioned in close proximity to the target, receives higher doses to achieve tumor control. Additionally, the comparison in our study was made with Tomotherapy, while previous studies compared 3D-CRT with IMRT. In fact, the reason for the higher EAR with the IMRT technique is the higher MU, the higher number of fields, and the larger volume of organs that are exposed to low-dose radiation [11, 22].

The small differences observed between the three biological models can be attributed to the use of dose per fraction < 2 Gy. At these low doses, the dose-response relationship is known to be linear, leading to similar results across the models. However, for higher doses and inhomogeneous dose distributions, the dose-response becomes non-linear, leading to potentially discrepancies between the models [39].

Figure 2 and Table 5 present Organ Equivalent Doses (OEDs) calculated using three methods: linear-exponential, plateau, and mechanistic. For the contralateral breast and lung, Tomotherapy generally delivered higher OEDs compared to 3D-CRT. However, this trend reversed for the

ipsilateral lung, where Tomotherapy yielded significantly lower OEDs. Notably, both techniques delivered higher OEDs to the ipsilateral lung compared to the contralateral counterparts, consistent with Han et al.'s findings [11].

The higher average MUs in IMRT compared to 3D-Conformal Radiation Therapy are caused by the increased modulation of multileaf collimators (MLCs). While this increased modulation can lead to higher doses to some organs, it likely contributed to the lower OEDs observed in the ipsilateral lung with Tomotherapy due to its improved dose fall-off and conformity compared to 3D-CRT.

While Haciislamoglu et al. [10] reported higher ipsilateral lung OEDs for IMRT and VMAT compared to 3D-CRT in their study, our findings differ, showing significantly lower OEDs in this region with Tomotherapy. This suggests that Tomotherapy, compared to other techniques, may offer greater control over dose delivery to organs near the target volume. This advantage could be attributed to Tomotherapy's unique delivery approach, involving rotating radiation beams that conform more closely to the target while minimizing dose spillover to surrounding structures.

Han et al. [11] compared Organ Equivalent Doses (OEDs) across five treatment modalities: 3D-CRT, Find, IMRT, VMAT, and TomoDirect, for several organs consist of the contralateral breast, contralateral lung, and ipsilateral lung. Their analysis revealed no significant differences in OED between most techniques, except for VMAT plans. VMAT plans exhibited higher OEDs to most critical structures, likely due to their larger irradiation volume.

The limitation of our study was that the evaluation of treatment planning for patients using three-dimensional (3D) techniques was performed retroactively. As a result, the investigator did not participate in contouring the target volume or approving the treatment plan. The treatment plans were performed by different physicists, and the target volume contouring and plan approval were performed by different radiation oncologists. Therefore, comparing them with the HT method, in which all target volume contours were performed by one person according to the RTOG guidelines, and plan approval was performed by one physicist and one radiation oncologist, can reduce its accuracy. Furthermore, a 5-millimeter margin was considered for the PTV in the design of HT treatment, so the treatment volume was larger than the 3D technique. This issue could lead to an increase in the dose received by organs at risk in tomotherapy.

Furthermore, the small size of sample should be noted. We used 10 patients for contouring and planning. Because of the limitation of the number of physicists who could plan both contouring and time limitation, we choose ten cases. It is recommended similar study to be run by larger sample size and similar methods.

It should be pointed out that this study does not report the actual incidence of secondary cancers in patients. Instead, it estimates the theoretical probability of secondary cancer occurrence based on radiation dose calculations. The patients were not followed up over a long period and the incidence of malignancies was not directly

observed. The data suggest the incidence of secondary cancer based on available formulations and theoretical dose calculations and it should be mentioned that the extent to which these theoretical estimations correspond to real-world clinical outcomes remains uncertain and requires long-term clinical follow-up studies with actual patient data to validate these models. Epidemiological studies have shown that there is a risk of secondary cancers following radiotherapy, but the precise magnitude of this risk and its direct correlation with the radiation dose to each organ need to be supported by longitudinal clinical data, which this study did not provided this follow up and this was not the main aim of this study.

In conclusion, a comparison of two treatment planning techniques, 3D-CRT and HT, in patients with left-sided breast cancer who were candidates for chest and regional lymph node radiation therapy, showed that the $D_{\rm max}$ to the heart, ipsilateral lung, spinal cord, and contralateral breast and the volume receiving a high dose ($V_{\rm 20}$ and $V_{\rm 30}$) of the heart and ipsilateral lung were significantly lower with HT. However, the volume receiving a low dose ($V_{\rm 5}$ and $V_{\rm 10}$) for all organs at risk except the ipsilateral lung, including the spinal cord, heart, thyroid, esophagus, lung, and contralateral breast, was significantly higher with HT. As a result, the EAR for the contralateral breast and lung was significantly higher with HT, but in the ipsilateral lung, the EAR was higher with 3D-CRT.

HT excels in precisely targeting the breast tumor while minimizing exposure to surrounding organs, particularly the heart and ipsilateral lung. This is particularly beneficial for patients with a high risk of cardiac complications or those who require higher doses of radiation to achieve tumor control.3D-CRT, on the other hand, offers superior control of dose to the contralateral breast and lung, which is crucial for minimizing the risk of secondary cancers and complications in these unaffected tissues. Given the distinct advantages of each technique, the ideal approach for each patient requires careful consideration of their individual circumstances and treatment goals. Incorporating individualized factors into the decisionmaking process ensures that the chosen radiation therapy technique aligns with the patient's best interests, balancing tumor control with minimizing potential side effects. Ultimately, the selection of the most suitable radiation therapy technique for breast cancer patients depends on a comprehensive assessment of the patient's unique characteristics and treatment goals.

Author Contribution Statement

Study concept and design: S.K. and N.H. Acquisition of data: N.H. Analysis and interpretation of data: N.H. Drafting of the manuscript: N.H. and S.K. and A.B.D. Critical revision of the manuscript for important content: S.K. Statistical analysis: A.M. Administrative, technical, and material support: A.B.D and N.H. Study supervision: S.K. and A.M.

Acknowledgements

There was no funding for this research and it was

part of an approved student thesis. Authors mention that there is no conflict of interest in this study. This study was a cross-sectional observational study. It was confirmed by the local committee of medical ethics, Shahid Beheshti University of Medical Science (Approval Code: IR.SBMU.MSP.REC.1399.577). The manuscript is original work of authors. All data, tables, figures, etc. used in the manuscript are prepared originally by authors, otherwise the sources are cited and reprint permission is attached. All the data are available on request of the journal with acceptable reason due to privacy of cases.

References

- 1. Becker SJ, Elliston C, Dewyngaert K, Jozsef G, Brenner D, Formenti S. Breast radiotherapy in the prone position primarily reduces the maximum out-of-field measured dose to the ipsilateral lung. Med Phys. 2012;39(5):2417-23. https://doi.org/10.1118/1.3700402.
- 2. Abo-Madyan Y, Aziz MH, Aly MM, Schneider F, Sperk E, Clausen S, et al. Second cancer risk after 3d-crt, imrt and vmat for breast cancer. Radiother Oncol. 2014;110(3):471-6. https://doi.org/10.1016/j.radonc.2013.12.002.
- Schneider U, Sumila M, Robotka J. Site-specific doseresponse relationships for cancer induction from the combined japanese a-bomb and hodgkin cohorts for doses relevant to radiotherapy. Theor Biol Med Model. 2011;8:27. https://doi.org/10.1186/1742-4682-8-27.
- Jemal A, Bray F, Center MM, Ferlay J, Ward E, Forman D. Global cancer statistics. CA Cancer J Clin. 2011;61(2):69-90. https://doi.org/10.3322/caac.20107.
- Schneider U, Zwahlen D, Ross D, Kaser-Hotz B. Estimation of radiation-induced cancer from three-dimensional dose distributions: Concept of organ equivalent dose. Int J Radiat Oncol Biol Phys. 2005;61(5):1510-5. https://doi. org/10.1016/j.ijrobp.2004.12.040.
- Grantzau T, Mellemkjær L, Overgaard J. Second primary cancers after adjuvant radiotherapy in early breast cancer patients: A national population based study under the danish breast cancer cooperative group (dbcg). Radiother Oncol. 2013;106(1):42-9. https://doi.org/10.1016/j. radonc.2013.01.002.
- Schubert LK, Gondi V, Sengbusch E, Westerly DC, Soisson ET, Paliwal BR, et al. Dosimetric comparison of left-sided whole breast irradiation with 3dcrt, forward-planned imrt, inverse-planned imrt, helical tomotherapy, and topotherapy. Radiother Oncol. 2011;100(2):241-6. https:// doi.org/10.1016/j.radonc.2011.01.004.
- Baycan D, Karacetin D, Balkanay AY, Barut Y. Field-in-field imrt versus 3d-crt of the breast. Cardiac vessels, ipsilateral lung, and contralateral breast absorbed doses in patients with left-sided lumpectomy: A dosimetric comparison. Jpn J Radiol. 2012;30(10):819-23. https://doi.org/10.1007/ s11604-012-0126-z.
- Zhang Q, Liu J, Ao N, Yu H, Peng Y, Ou L, et al. Secondary cancer risk after radiation therapy for breast cancer with different radiotherapy techniques. Sci Rep. 2020;10(1):1220. https://doi.org/10.1038/s41598-020-58134-z.
- 10. Haciislamoglu E, Cinar Y, Gurcan F, Canyilmaz E, Gungor G, Yoney A. Secondary cancer risk after whole-breast radiation therapy: Field-in-field versus intensity modulated radiation therapy versus volumetric modulated arc therapy. Br J Radiol. 2019;92(1102):20190317. https://doi.org/10.1259/bjr.20190317.
- 11. Han EY, Paudel N, Sung J, Yoon M, Chung WK, Kim DW. Estimation of the risk of secondary malignancy

- arising from whole-breast irradiation: Comparison of five radiotherapy modalities, including tomohda. Oncotarget. 2016;7(16):22960-9. https://doi.org/10.18632/oncotarget.8392.
- 12. Haciislamoglu E, Colak F, Canyilmaz E, Dirican B, Gurdalli S, Yilmaz AH, et al. Dosimetric comparison of left-sided whole-breast irradiation with 3dcrt, forward-planned imrt, inverse-planned imrt, helical tomotherapy, and volumetric arc therapy. Phys Med. 2015;31(4):360-7. https://doi.org/10.1016/j.ejmp.2015.02.005.
- 13. Hall EJ. Intensity-modulated radiation therapy, protons, and the risk of second cancers. Int J Radiat Oncol Biol Phys. 2006;65(1):1-7. https://doi.org/10.1016/j.ijrobp.2006.01.027.
- Xu XG, Bednarz B, Paganetti H. A review of dosimetry studies on external-beam radiation treatment with respect to second cancer induction. Phys Med Biol. 2008;53(13):R193-241. https://doi.org/10.1088/0031-9155/53/13/r01.
- Kourinou KM, Mazonakis M, Lyraraki E, Stratakis J, Damilakis J. Scattered dose to radiosensitive organs and associated risk for cancer development from head and neck radiotherapy in pediatric patients. Phys Med. 2013;29(6):650-5. https://doi.org/10.1016/j.ejmp.2012.08.001.
- 16. Joosten A, Matzinger O, Jeanneret-Sozzi W, Bochud F, Moeckli R. Evaluation of organ-specific peripheral doses after 2-dimensional, 3-dimensional and hybrid intensity modulated radiation therapy for breast cancer based on monte carlo and convolution/superposition algorithms: Implications for secondary cancer risk assessment. Radiother Oncol. 2013;106(1):33-41. https://doi.org/10.1016/j.radonc.2012.11.012.
- 17. Diallo I, Haddy N, Adjadj E, Samand A, Quiniou E, Chavaudra J, et al. Frequency distribution of second solid cancer locations in relation to the irradiated volume among 115 patients treated for childhood cancer. Int J Radiat Oncol Biol Phys. 2009;74(3):876-83. https://doi.org/10.1016/j.ijrobp.2009.01.040.
- 18. Murray LJ, Thompson CM, Lilley J, Cosgrove V, Franks K, Sebag-Montefiore D, et al. Radiation-induced second primary cancer risks from modern external beam radiotherapy for early prostate cancer: Impact of stereotactic ablative radiotherapy (sabr), volumetric modulated arc therapy (vmat) and flattening filter free (fff) radiotherapy. Phys Med Biol. 2015;60(3):1237-57. https://doi.org/10.1088/0031-9155/60/3/1237.
- Zhang Q, Zeng Y, Peng Y, Yu H, Zhang S, Wu S. Critical evaluation of secondary cancer risk after breast radiation therapy with hybrid radiotherapy techniques. Breast Cancer (Dove Med Press). 2023;15:25-38. https://doi.org/10.2147/ bctt.S383369.
- Haertl PM, Pohl F, Weidner K, Groeger C, Koelbl O, Dobler B. Treatment of left sided breast cancer for a patient with funnel chest: Volumetric-modulated arc therapy vs. 3d-crt and intensity-modulated radiotherapy. Med Dosim. 2013;38(1):1-4. https://doi.org/10.1016/j. meddos.2012.04.003.
- 21. Jin GH, Chen LX, Deng XW, Liu XW, Huang Y, Huang XB. A comparative dosimetric study for treating left-sided breast cancer for small breast size using five different radiotherapy techniques: Conventional tangential field, filed-in-filed, tangential-imrt, multi-beam imrt and vmat. Radiat Oncol. 2013;8:89. https://doi.org/10.1186/1748-717x-8-89.
- 22. Lee B, Lee S, Sung J, Yoon M. Radiotherapy-induced secondary cancer risk for breast cancer: 3d conformal therapy versus imrt versus vmat. J Radiol Prot. 2014;34(2):325-31. https://doi.org/10.1088/0952-4746/34/2/325.
- 23. Vii BE. Health risks from exposure to low levels of ionizing

- radiation. The National Academies report in brief. 2005.
- Paddick I. A simple scoring ratio to index the conformity of radiosurgical treatment plans. Technical note. J Neurosurg. 2000;93 Suppl 3:219-22. https://doi.org/10.3171/ jns.2000.93.supplement.
- 25. Murthy V, Mallik S, Master Z, Sharma PK, Mahantshetty U, Shrivastava SK. Does helical tomotherapy improve dose conformity and normal tissue sparing compared to conventional imrt? A dosimetric comparison in high risk prostate cancer. Technol Cancer Res Treat. 2011;10(2):179-85. https://doi.org/10.7785/tcrt.2012.500193.
- 26. Lee JW, Hong S, Choi KS, Kim YL, Park BM, Chung JB, et al. Performance evaluation of field-in-field technique for tangential breast irradiation. Jpn J Clin Oncol. 2008;38(2):158-63. https://doi.org/10.1093/jjco/hym167.
- 27. Furuya T, Sugimoto S, Kurokawa C, Ozawa S, Karasawa K, Sasai K. The dosimetric impact of respiratory breast movement and daily setup error on tangential whole breast irradiation using conventional wedge, field-in-field and irregular surface compensator techniques. J Radiat Res. 2013;54(1):157-65. https://doi.org/10.1093/jrr/rrs064.
- 28. Verhaegen F, Seuntjens J. Monte carlo modelling of external radiotherapy photon beams. Phys Med Biol. 2003;48(21):R107-64. https://doi.org/10.1088/0031-9155/48/21/r01.
- Howell RM, Scarboro SB, Kry SF, Yaldo DZ. Accuracy of out-of-field dose calculations by a commercial treatment planning system. Phys Med Biol. 2010;55(23):6999-7008. https://doi.org/10.1088/0031-9155/55/23/s03.
- 30. Hasenbalg F, Neuenschwander H, Mini R, Born EJ. Collapsed cone convolution and analytical anisotropic algorithm dose calculations compared to vmc++ monte carlo simulations in clinical cases. Phys Med Biol. 2007;52(13):3679-91. https:// doi.org/10.1088/0031-9155/52/13/002.
- Krieger T, Sauer OA. Monte carlo- versus pencil-beam-/ collapsed-cone-dose calculation in a heterogeneous multilayer phantom. Phys Med Biol. 2005;50(5):859-68. https:// doi.org/10.1088/0031-9155/50/5/010.
- Alzoubi AS, Kandaiya S, Shukri A, Elsherbieny E. Contralateral breast dose from chest wall and breast irradiation: Local experience. Australas Phys Eng Sci Med. 2010;33(2):137-44. https://doi.org/10.1007/s13246-010-0011-y.
- Xie Y, Bourgeois D, Guo B, Zhang R. Comparison of conventional and advanced radiotherapy techniques for left-sided breast cancer after breast conserving surgery. Med Dosim. 2020;45(4):e9-e16. https://doi.org/10.1016/j. meddos.2020.05.004.
- 34. Willner J, Jost A, Baier K, Flentje M. A little to a lot or a lot to a little? An analysis of pneumonitis risk from dose-volume histogram parameters of the lung in patients with lung cancer treated with 3-D conformal radiotherapy. Strahlentherapie und Onkologie. 2003;179(8):548-56.
- 35. Roeder F, Friedrich J, Timke C, Kappes J, Huber P, Krempien R, et al. Correlation of patient-related factors and dose-volume histogram parameters with the onset of radiation pneumonitis in patients with small cell lung cancer. Strahlenther Onkol. 2010;186(3):149-56. https://doi.org/10.1007/s00066-010-2018-4.
- 36. Dang J, Li G, Zang S, Zhang S, Yao L. Risk and predictors for early radiation pneumonitis in patients with stage iii nonsmall cell lung cancer treated with concurrent or sequential chemoradiotherapy. Radiat Oncol. 2014;9:172. https://doi. org/10.1186/1748-717x-9-172.
- 37. Blom Goldman U, Wennberg B, Svane G, Bylund H, Lind P. Reduction of radiation pneumonitis by v20-constraints in breast cancer. Radiat Oncol. 2010;5:99. https://doi.

- org/10.1186/1748-717x-5-99.
- 38. Moon SH, Shin KH, Kim TH, Yoon M, Park S, Lee DH, et al. Dosimetric comparison of four different external beam partial breast irradiation techniques: Three-dimensional conformal radiotherapy, intensity-modulated radiotherapy, helical tomotherapy, and proton beam therapy. Radiother Oncol. 2009;90(1):66-73. https://doi.org/10.1016/j. radonc.2008.09.027.
- 39. Hall EJ, Wuu CS. Radiation-induced second cancers: The impact of 3d-crt and imrt. Int J Radiat Oncol Biol Phys. 2003;56(1):83-8. https://doi.org/10.1016/s0360-3016(03)00073-7.



This work is licensed under a Creative Commons Attribution-Non Commercial 4.0 International License.